Mon. Not. R. Astron. Soc. 000, 1–9 (1998) Printed 19 October 1998 (MN LATEX style file v1.4)

[C II] 158 μm observations of a sample of late-type galaxies from the Virgo cluster

K. J. Leech,[1] H.J. Völk,[2] I. Heinrichsen,[1,2,4] H. Hippelein,[3] L. Metcalfe,[1] D. Pierini,[2] C.C. Popescu,[2] R.J. Tuffs[2] and C. Xu[4]

[1] *ESA Villafranca, P.O. Box 50727, Madrid, Spain*

[2] *Max-Planck-Institut für Kernphysik, Heidelberg, Germany*

[3] *Max-Planck-Institut für Astronomie, Heidelberg, Germany*

[4] *IPAC, Caltech, USA*

Accepted 1988 December 15. Received 1988 December 14; in original form 1988 October 11

ABSTRACT

We have observed 19 **Virgo cluster** spiral galaxies with the **Long Wavelength Spectrometer (LWS)** onboard ESAs **Infrared Space Observatory (ISO)** obtaining spectra around the [C II] 157.741 μm fine structure line. These 19 galaxies are quiescent, sample RC3 types 0 to 8 and come from both the cluster core and the cluster periphery. The sample enables us to probe any difference in the [C II] emission between different RC3 types or between core and periphery galaxies.

Of the 19 galaxies, which are are relatively quiescent in star forming activity compared to previous studies from airborne observatories, 15 were detected in the [CII] line. Any influence of the Virgo cluster enviroment on the [CII] emission was found to be small compared with the stong dependence of the line emission on basic measurables such as morphology or stellar mass. While the range of the [C II] to FIR ratio is less than in other surveys (reflecting the fact these galaxies are relatively quiescent), there is a good correlation between the strength of the [C II] line and the Far-IR flux, as measured by IRAS. Of interest is the order of magnitude difference in

1 INTRODUCTION

The ISO ((Kessler *et al.* (1996))) Guaranteed Time programme VIRGO, (Völk *et al. in prep*), is a study of a complete volume-limited, unbiased sample of spiral, irregular and BCD galaxies from the Virgo cluster, selected from the Virgo Cluster Catalogue (VCC) of (Binggeli *et al.* (1985)), as described in (Boselli *et al.* (1997)). The selection criteria used to define this sample will be discussed in (Völk *et al. in prep*). While the VIRGO proposal is primarily photometric, we wished to observe many of these galaxies spectroscopically. Various constraints limited observations to the [C II] 157.741 μm cooling line. This line should probe photodissociation regions (cf. (Stacey *et al.* (1991))) associated with massive star formation, and also the diffuse components of the Interstellar Medium (e.g. (Nakagawa *et al.* (1998))). It has been observed not only in "compact" regions of the Galaxy like HII regions, OB associations, reflection nebulae, and planetary nebulae, but also in "diffuse" regions, as well as for for entire galaxies. [C II] emission is thought to be the most important gas cooling process in late type galaxies, balancing the photoelectric heating from grains.

While in field galaxies the [C II] line has a luminosity of the order of 10^{-3} to 10^{-2} that of the total FIR flux of a galaxy (e.g. (Malhotra *et al.* (1997))), the Virgo sample – even the top end of the luminosity range observed – is less active in star forming activity that the field sample of (Malhotra *et al.* (1997)). Indeed the need to get a deep sample embracing quiescent galaxies was the fundamental motivation for observing Virgo galaxies.

At the distance of the Virgo cluster (taken to be 15 covers and area of approximately 7 kpc in diameter – optical images of the Virgo galaxies by (Sandage, Binggeli & Tammann (1985)) indicate that the LWS beam covers out to the observed spiral arms. The extended [C II] emission detected at this distance in NGC 6946 by (Madden *et al.* (1993)) accounted for 70% of the total [C II] emission. Observation of Virgo galaxies with LWS will therefore detect not only [C II] emission from the dense nucleus but, assuming Virgo galaxies are similar to NGC 6946, will primarily sample the [C II] emission from diffuse regions in and between the spiral arms.

The prime reasons for choosing the sample from the Virgo cluster for this detection survey was the high level of completeness of the VCC, (to B_T 18), and because at the distance to the cluster the typical angular sizes of the IR emitting regions are well matched to the angular resolution of ISO. Nevertheless, the question as to whether there was any difference between the conditions in the core of the Virgo cluster and its periphery was also of interest.

This paper presents a preliminary reduction, analysis and discussion of the [C II] data. Five VCC galaxies observed around the [C II] line by (Smith & Madden (1997)) are combined to produce a slightly larger sample. A further paper, ((Pierini *et al.* (1998))), discusses the [C II] data in more detail and its relation to other measures of the star-forming activity.

2 SAMPLE SELECTION AND OBSERVATIONS

A subsample of Virgo galaxies, bright enough to be observed with the Long Wavelength Spectrometer (LWS), (Clegg *et*

of the [C II] line (based on the integrated Blue magnitude), the sensitivity of LWS and the time available. VCC core galaxies with an integrated blue magnitude, Bt, $\leq$ 12.6 and periphery galaxies with Bt $\leq$ 12.0 were selected. Core galaxies were defined to be those within 2 degrees of M87 and periphery galaxies defined to be those more than 4 degrees from the position of maximum galaxy surface density, and these criteria are discussed in (Boselli *et al.* (1997)). The different magnitude limits were chosen to select approximately equal numbers of core and periphery galaxies and resulted in 12 core galaxies and 11 periphery galaxies being selected. Of these 23 galaxies, four (3 core and 1 periphery) could not be observed as they were part of another programme, and one (faint) core galaxy could not be observed due to time constraints.

One other optically faint core galaxy, VCC 1326, was observed to serve as a cross-calibration target between the LWS measurements and the ISOPHOT ((Lemke *et al.* (1996))) measurements of the larger VIRGO programme. VCC 1326 is in some respects an atypical VCC galaxy as it is faint in the optical and yet was selected to be bright in the IR so as to be detected by LWS and PHOT. It provides a useful photometric comparison between the LWS measurements and the PHOT measurements of (Völk *et al. in prep*).

Information on all these galaxies is given in Table 1, together with the positions of sky background reference fields (denoted VBACK in the following tables and figures) to check for foreground [C II] emission from the Milky Way.

The observing log is given in Table 2. All observations carried out were standard grating range scans (AOT 2's),

Table 2. *Observing log.*

Target	Date Observed	Observation set
VCC 66	12 July	8
VCC 92	9 July	1
VCC 460	8 July	2
VCC 857	8 July	2
VCC 873	4 July	4
VCC 1003	5 July	5
VCC 1043	5 July	4
VCC 1110	8 July	2
VCC 1158	4 July	4
VCC 1253	4 July	4
VCC 1326	5 July	5
VCC 1412	5 July	5
VCC 1690	5 July	4
VCC 1727	15 July	6
VCC 1813	15 July	6
VCC 1869	15 July	6
VCC 1972	15 July	6
VCC 1987	30 June	3
VCC 2070	15 July	7
VBACK01	9 July	1
VBACK03	12 July	8
VBACK04	8 July	2
VBACK12_1	15 July	6
VBACK12_2	15 July	7
VBACK13	30 June	3

ies in sequence (in ISO terminology, the observations were concatenated), with one sky background position used for each set. The observation set number is indicated in the table. All observations were made between 30^{th} June and 15^{th} July 1996 with no problems reported.

3 DATA REDUCTION AND RESULTS

The Auto Analysis Results from Off-Line Processing (OLP) version 6 were processed further using the ISO Spectral Analysis Package (ISAP) by: reading data in; discarding bad LWS data points; averaging scans for detector 8 (the one covering the 158 μm region); and finally fitting continua and gaussians to any lines seen in the data to obtain flux and central wavelength.

Table 1. *Sample galaxies and positions of selected reference fields.*

Target	Alternate name	RA (J2000)	DEC (J2000)	Core or Periphery	60 μm flux (Jy)	100 μm flux (Jy)	B_T
VCC 66	NGC 4178	12 12 46.9	10 52 07.0	P	2.8	9.0	11.9
VCC 92	NGC 4192,M98	12 13 48.4	14 54 07.2	P	6.5	21.5	10.9
VCC 460	NGC 4293	12 21 13.2	18 23 03.6	P	4.6	10.6	11.2
VCC 857	NGC 4394	12 25 56.0	18 12 47.6	P	1.0	4.3	11.8
VCC 873	NGC 4402	12 26 06.8	13 06 47.6	C	5.4	17.4	12.6
VCC 1003	NGC 4429	12 27 26.2	11 06 30.3	C	1.4	4.3	11.1
VCC 1043	NGC 4438	12 27 45.7	13 00 30.4	C	3.7	13.1	10.9
VCC 1110	NGC 4450	12 28 29.5	17 05 06.8	P	1.4	7.6	10.9
VCC 1158	NGC 4461	12 29 03.0	13 11 07.1	C	<0.2	<0.8	12.1
VCC 1253	NGC 4477	12 30 02.9	13 38 07.7	C	0.5	1.0	11.3
VCC 1326	NGC 4491	12 30 57.2	11 29 02.1	C	2.8	3.3	13.4
VCC 1412	NGC 4503	12 32 05.5	11 10 38.8	C	<0.2	1.0	12.1
VCC 1690	NGC 4569,M90	12 36 49.9	13 09 53.8	C	8.8	25.0	10.2
VCC 1727	NGC 4579	12 37 43.5	11 49 06.4	C	4.9	19.6	10.6
VCC 1813	NGC 4596	12 39 56.3	10 10 38.0	P	0.4	1.0	11.5
VCC 1869	NGC 4608	12 41 13.6	10 09 14.9	P	<0.2	<0.5	12.0
VCC 1972	NGC 4647	12 43 32.4	11 34 46.7	P	4.9	15.9	12.0
VCC 1987	NGC 4654	12 43 57.2	13 07 35.1	P	13.4	33.4	11.1
VCC 2070	NGC 4698	12 48 23.2	8 29 14.9	P	<0.2	1.6	11.5
VBACK01		12 13 30.9	15 30 47.2				
VBACK03		12 13 52.4	8 29 12.2				
VBACK04		12 25 05.9	17 43 52.1				
VBACK12_1		12 43 08.5	9 47 34.4				
VBACK12_2		12 43 08.5	9 47 34.4				
VBACK13		12 48 14.5	12 58 38.7				

six background positions used, five had no detectable emission at galactic [C II] wavelengths and one was repointed to VCC 873 (confirming the line flux and wavelength for that galaxy). In several galaxy observations (e.g. VCC 1110) galactic [C II] emission was observed, and in all such cases was measured and noted. In only one case do we think there may be confusion between emission from galactic [C II] and the target Virgo galaxy (VCC 1326) - this is discussed later.

The [C II] line wavelength region for all galaxies are shown in figures 1 to 5, and background positions are shown in figures 6 and 7. A few of the observations suffer from memory effects and/or glitches that cause the first few short-wavelength datapoints to be systematically lower than the line or continuum fluxes. In all cases the baselines are arbitrary, but can be derived from Table 3.

Line fluxes, central wavelengths and continuum fluxes are given in Table 3. In cases where no line was present the strongest feature in the spectral region was taken to be the upper limit of detectability. In Table 3 the errors quoted for the lines and continuum are statistical and do not include any errors due to, e.g., memory effects or flux calibration errors. A better guide to the errors can be obtained by comparing the two observations of VCC 873. The line fluxes agree to high precision whereas the continuum fluxes differ

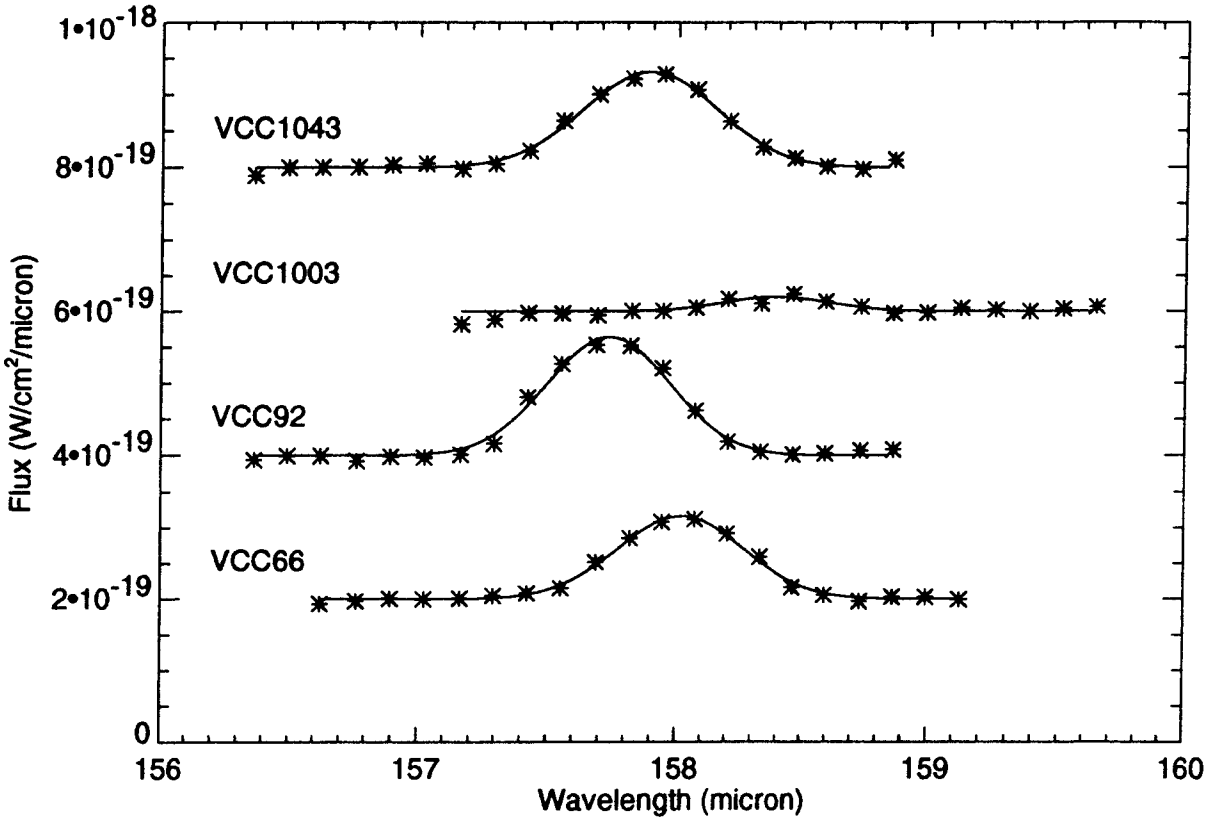

Figure 1. Virgo galaxy set 1

Table 4. *Galaxies observed added to this sample*

Target name	Alternate name	B_T	[C II] Line flux W/cm^2	L(FIR) $L_\odot$
VCC 89	NGC 4189	12.1	$9.1 \pm 0.8 \times 10^{-20}$	2.7×10^9
VCC 187	NGC 4222	12.7	$4.5 \pm 0.9 \times 10^{-20}$	9.0×10^8
VCC 465	NGC 4294	11.8	$8.4 \pm 0.9 \times 10^{-20}$	1.9×10^9
VCC 491	NGC 4299	12.7	$6.8 \pm 0.9 \times 10^{-20}$	1.7×10^9
VCC 1516	NGC 4522	12.0	$8.1 \pm 0.9 \times 10^{-20}$	1.3×10^9

4 DISCUSSION

To this sample of 19 galaxies we can also add the five galaxies observed by (Smith & Madden (1997)), a summary of the important information being given in Table 4.

Figure 9 shows the relation between the [C II] flux and the FIR flux from IRAS measurements given by $FIR =$ *et al.* (1988))). Despite the spatial mis-match between the LWS 80 arcsec diameter circular aperture and the larger IRAS square apertures, there is a good correlation between these observed quantities despite the approximately two orders of magnitude range in both observable quantities.

Figure 8 shows the [C II] to FIR ratio against the dust temperature, as measured by the ratio of the IRAS flux densities at 60 and 100 μm. When detected, the [C II] to FIR ratio ranges from 0.1% to 0.5%. This covers the ranges expected for compact sources (0.2%), such as active star-forming regions, to the diffuse component on the ISM (0.6%), (Nakagawa *et al.* (1998)). Galaxies observed by (Stacey *et al.* (1991)) cover the range 0.15 - 0.6% and in

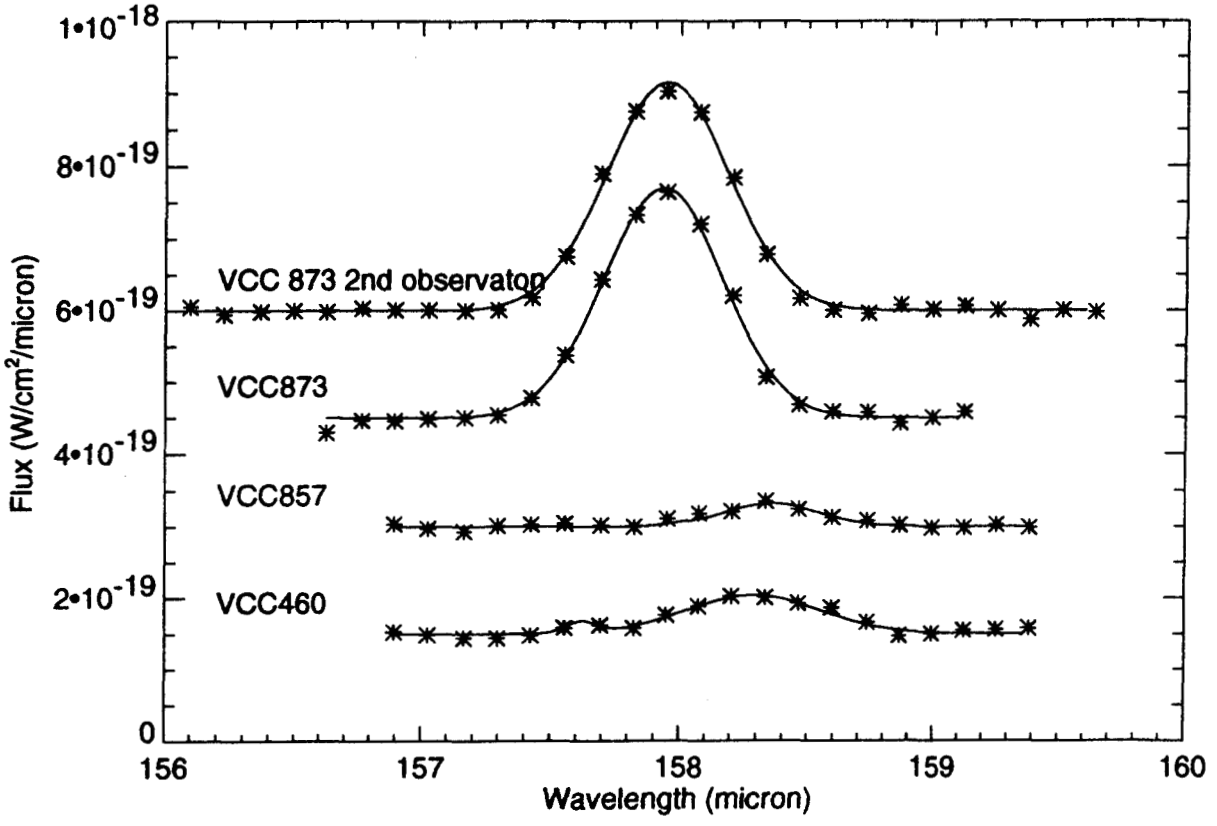

Figure 2. Virgo galaxy set 2

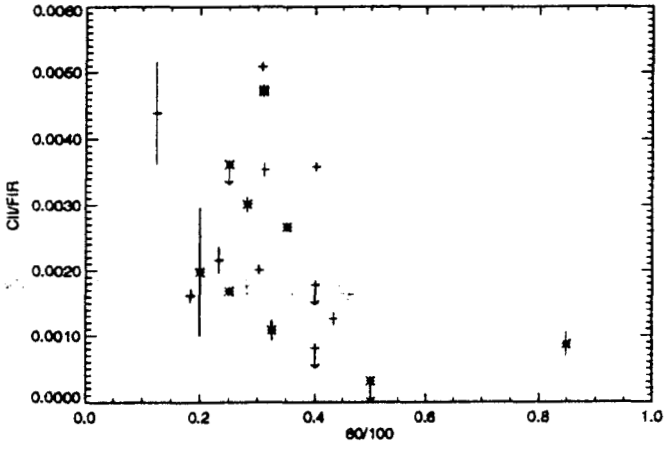

Figure 8. [C II]/FIR ratio against dust temperature, indicated by 60/100 μm ratio. Error bars and upper limits are marked. Core galaxies are marked by '*', periphery by '+'.

terest in this plot are two galaxies with $60/100 > 0.5$ with apparently anomalously low [C II]/FIR ratios.

VCC 1326 has a 60/100 ratio of 0.85 and a [C II]/FIR

the range of observed values in (Malhotra *et al.* (1997)). It is the faintest galaxy in our sample, with a B_T magnitude of 13.4. Interestingly, it has enhanced X-ray emission with respect to the hot Intracluster Medium ((Ohashi & Kikuchi (1997))). There is the possibility that the [C II] emission from VCC 1326 is confused with that from galactic foreground emission, making the [C II]/FIR ratio even lower. The expected [C II] emission wavelength of 157.92 μmis very close to that of galactic emission. While the strength of the emission, 1.2×10^{-20} W cm^{-2}, is only just greater than one background measurement (that of VCC 1972), is several times that the average background and we therefore do not expect it to be heavily contaminated by galactic emis-

sion

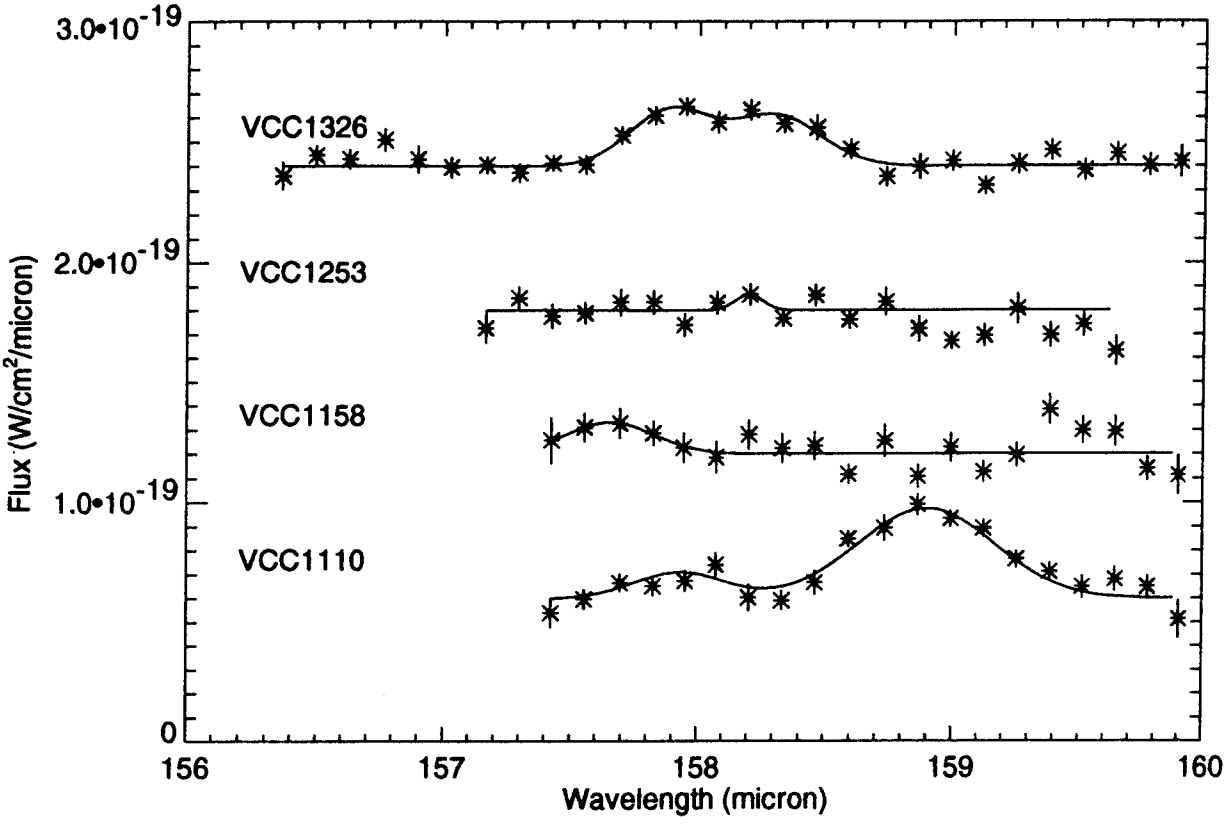

Figure 3. Virgo galaxy set 3

detection. This gives it a very low [C II]/FIR ratio, placing it outside the normal galaxy region of (Malhotra *et al.* (1997)). The optical spectrum of this galaxy given in (Ho *et al.* (1988)) show it to be a normal starburst galaxy, and its IR fluxes or B magnitude (see Table 1) are normal. However, it shows an asymetric inner region in the K*l*-band image of Boselli et al. (1997).

The [C II] to FIR ratio for these galaxies lies in the range $\approx$ 0.001 to 0.005 when detected, and for one galaxy an upper limit of 0.0005 can be determined. This range is not unusual, as galaxies observed by (Stacey *et al.* (1991)) covered the range 0.0015 - 0.006, and in NGC 5713 the ratio is 0.007, but the upper limit is very low.

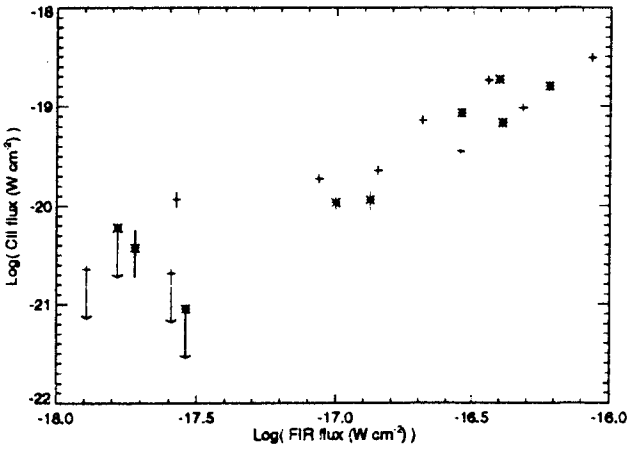

Figure 9. [C II] flux against FIR flux. Error bars are marked in the vertical, where they are larger than the symbol size, and upper limits are marked. Core galaxies are marked by '*', periphery by '+'.

Although statistics are poor and there are large intrinsic

show an overall linear correlation between [C II] and dust

continuum luminosity. They are broadly consistent with the

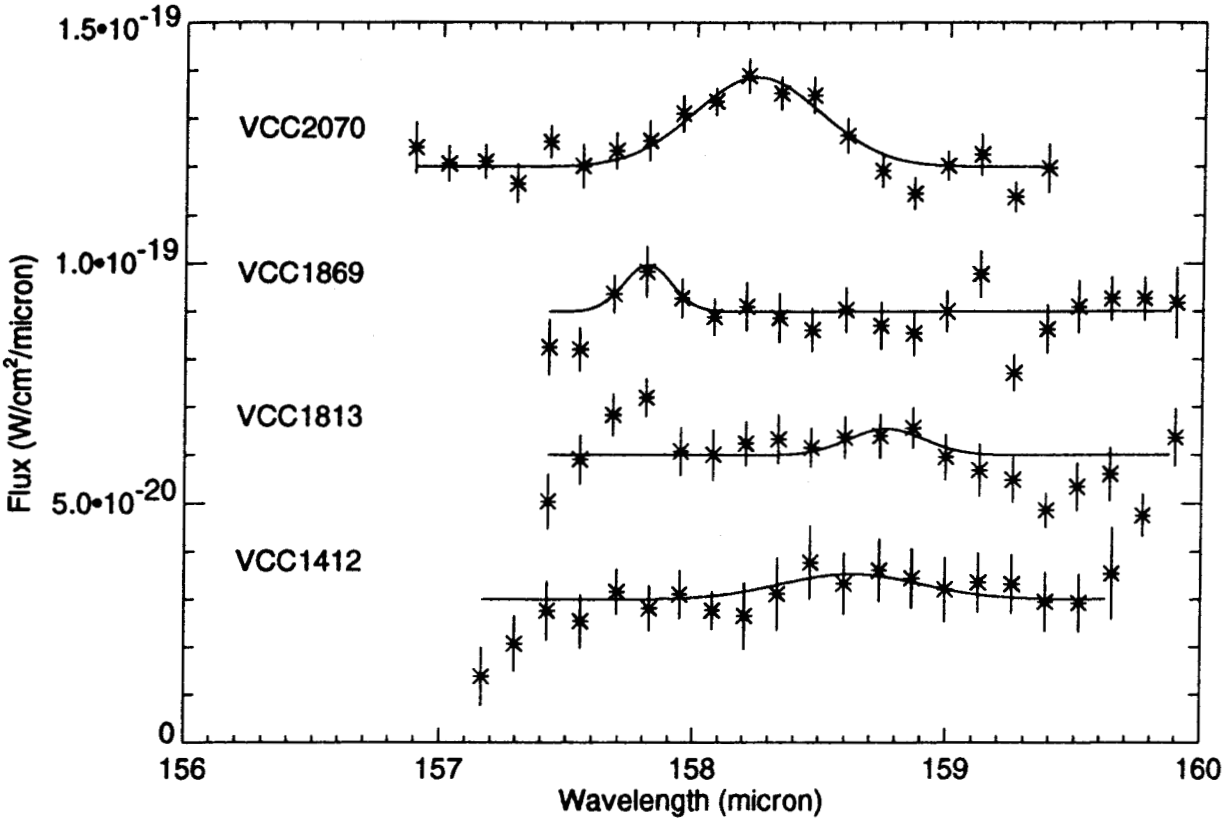

Figure 4. Virgo galaxy set 4

by (Smith & Madden (1997)). Galaxies which have higher continuum and line brightnesses tend to have later Hubble types. This is consistent with the increase in star formation activity with increasing lateness , e.g. (Kennicutt *et al.* (1994)). The tendency for the correlation to flatten off with increasing brightness, as observed by (Stacey *et al.* (1991)) for a sample embracing starburst and ultraluminous galaxies, is not apparent for the relatively quiescent Virgo sample. There is no apparent relation between the [C II] line/dust colour ratio and position in the cluster or HI mass surface density in the galaxian disks. Therefore, any relation of the [C II] emission to the diffuse HI component of the ISM is not obvious, at least for the central regions of the disks observed.

5 CONCLUSION

We have observed 19 galaxies with the LWS spectrometer onboard the ISO satellite around the [C II] fine structure line, detecting 15 of these. A good correlation is found between the strength of the [C II] and the FIR flux. Both fluxes increase significantly with later Hubble types. Conversely, no difference can be found in the [C II] properties between the core and periphery galaxies.

One galaxy, VCC 1253, has an abnormally low [C II] strength. Further observations of this unusual galaxy are warranted.

REFERENCES

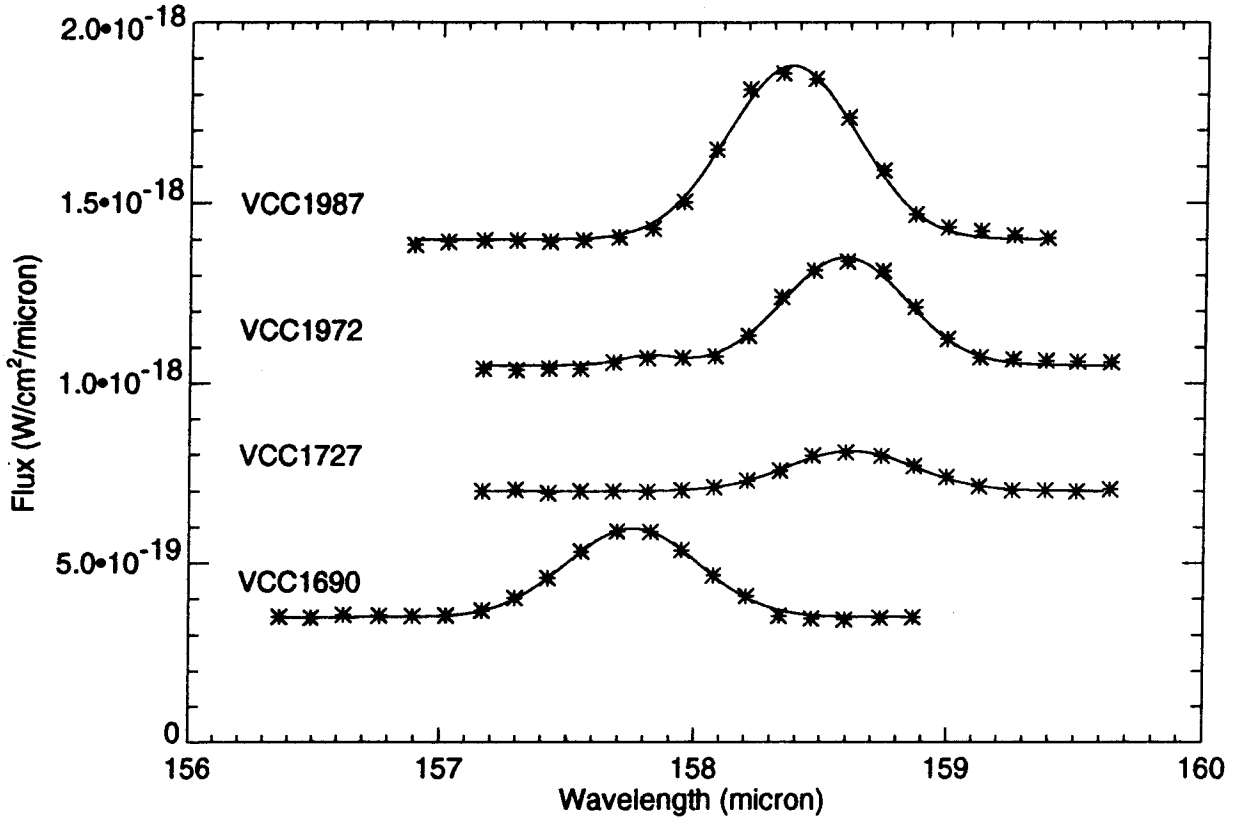

Figure 5. Virgo galaxy set 5

Boselli A., *et al.* 1997, AA Supp 121, 507

Clegg, P.E *et al.* 1996, A&A 315, L38

Helou G., *et al.* 1988, ApJS 68, 151.

Ho, L., *et al.* 1995, ApJS 98, 477

Kennicutt, R.C., Tamblyn, P., Congdon, C., 1994, ApJ 435, 22

Kessler, M.F. *et al.* 1996, A&A 315, L27

Lemke, D. *et al.* 1996, A&A 315, L64.

Lord, S.D. *et al.* 1996 A&A, 315, L117.

Madden, S.C. *et al.* 1993, ApJ 407, 579.

Malhotra, S., *et al.* 1997 ApJ 491, L27.

Nakagawa, T., *et al.* 1998 ApJS 115, 259.

Ohashi, T., & Kikuchi, K. 1997, IAU 188, 148

Pierini, D. *et al.* 1998, A&A *submitted*

Sandage, A., Binggeli B., Tammann G.A. 1985, AJ 90, 395.

Smith, B.J., Madden, S.C. 1997 AJ 114, 138

Völk, H., *et al.* 1998, *in prep*

ACKNOWLEDGEMENTS

This paper is based on observations with the Infrared Space Observatory (ISO). ISO is an ESA project with instruments funded by ESA member states (especially the PI countries: France, Germany, the Netherlands and the United Kingdom) and with the participation of ISAS and NASA.

The ISO Spectral Analysis Package (ISAP) is a joint development by the LWS and SWS Instrument Teams and Data Centres. Contributing institutes are CESR, IAS, IPAC, MPE, RAL and SRON.

This paper has been produced using the Royal Astronomical

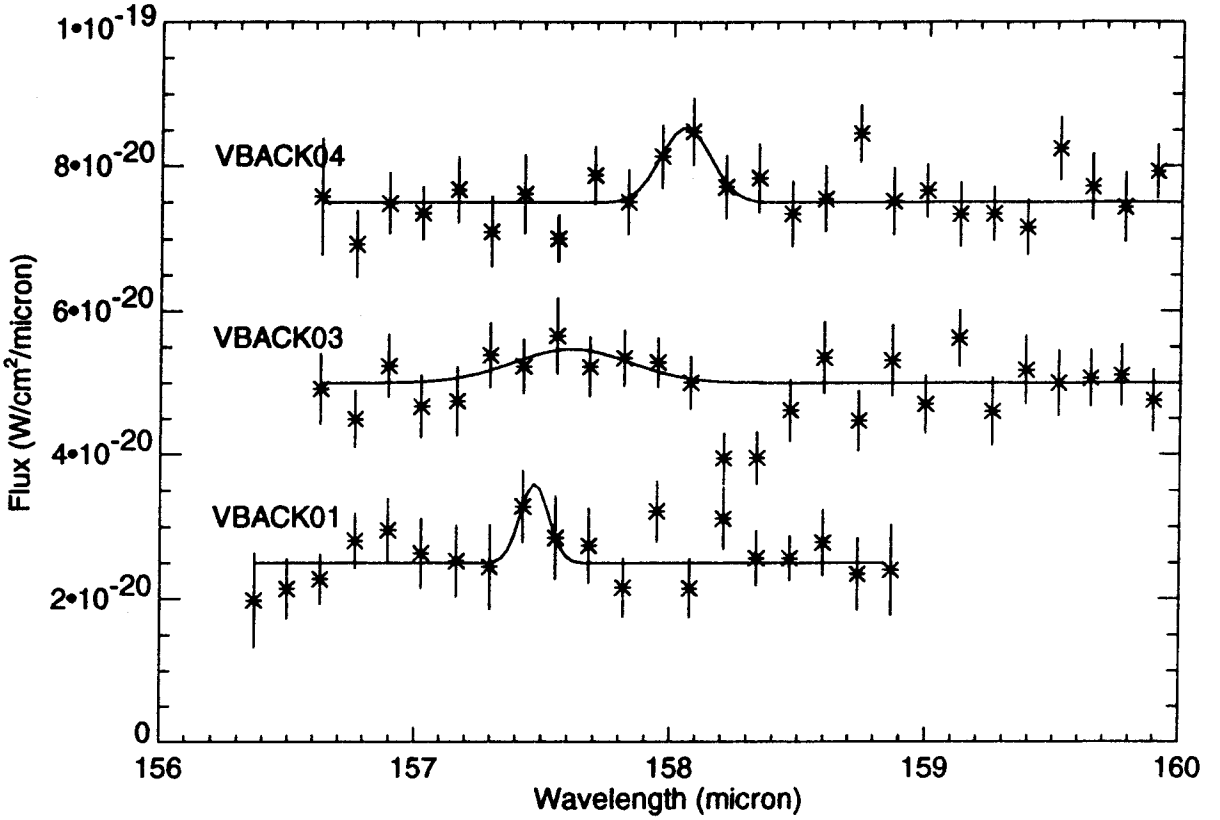

Figure 6. First set of Background observations

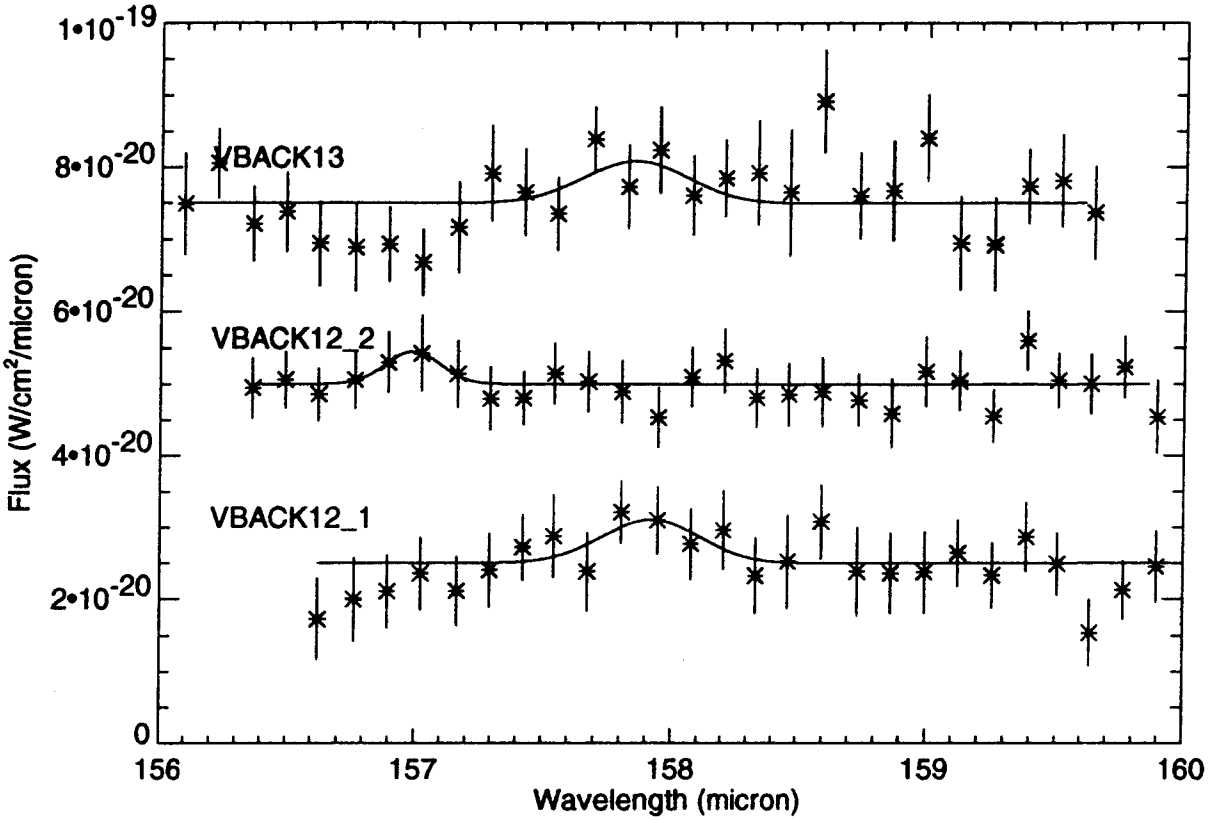

Figure 7. Second set of Background observations

Table 3. *Results*

Target name	Continuum flux $W/cm^2/\mu m$	Line FWHM km/s	Line flux W/cm^2	Line Wavelength μm	Note
VCC 66	$4.3 \pm 0.1 \times 10^{-20}$	1110.5	$7.2 \pm 0.2 \times 10^{-20}$	158.022 ± 0.006	
VCC 92	$1.73 \pm 0.01 \times 10^{-19}$	1057.2	$9.7 \pm 0.2 \times 10^{-20}$	157.736 ± 0.003	
VCC 460	$1.17 \pm 0.01 \times 10^{-19}$	1180.4	$3.6 \pm 0.3 \times 10^{-20}$	158.29 ± 0.02	
		597.1	$4.7 \pm 2.1 \times 10^{-21}$	157.69 ± 0.04	g
VCC 857	$6.1 \pm 0.1 \times 10^{-20}$	1065.0	$1.9 \pm 0.2 \times 10^{-20}$	158.32 ± 0.02	
		848.8	$3.0 \pm 1.8 \times 10^{-21}$	157.51 ± 0.08	g
VCC 873	$2.19 \pm 0.02 \times 10^{-19}$	1035.7	$1.86 \pm 0.03 \times 10^{-19}$	157.932 ± 0.003	
VCC 873	$1.88 \pm 0.01 \times 10^{-19}$	1056.3	$1.87 \pm 0.03 \times 10^{-19}$	157.947 ± 0.003	2
VCC 1003	$4.85 \pm 0.09 \times 10^{-20}$	961.2	$1.1 \pm 0.1 \times 10^{-20}$	158.39 ± 0.02	
VCC 1043	$1.23 \pm 0.02 \times 10^{-19}$	1166.9	$8.6 \pm 0.3 \times 10^{-20}$	157.890 ± 0.008	
VCC 1110	$8.5 \pm 0.1 \times 10^{-20}$	1125.2	$2.3 \pm 0.1 \times 10^{-20}$	158.89 ± 0.01	
		935.6	$5.8 \pm 1.3 \times 10^{-21}$	157.92 ± 0.03	g
VCC 1158	$1.3 \pm 0.2 \times 10^{-20}$	774.8	$6 \pm 4 \times 10^{-21}$	157.65 ± 0.08	u
VCC 1253	$1.6 \pm 1.3 \times 10^{-21}$	241.5	$0.9 \pm 1.6 \times 10^{-21}$	158.2	u
VCC 1326	$4.1 \pm 0.1 \times 10^{-20}$	819.8	$1.2 \pm 0.3 \times 10^{-20}$	157.92 ± 0.03	
VCC 1412	$2.00 \pm 0.08 \times 10^{-20}$	1243.5	$3.8 \pm 1.9 \times 10^{-21}$	158.6 ± 0.1	
VCC 1690	$2.70 \pm 0.01 \times 10^{-19}$	1152.0	$1.60 \pm 0.02 \times 10^{-19}$	157.755 ± 0.003	
VCC 1727	$1.14 \pm 0.01 \times 10^{-19}$	1110.6	$6.9 \pm 0.2 \times 10^{-20}$	158.614 ± 0.005	
VCC 1813	$1.01 \pm 0.02 \times 10^{-20}$	668.3	$2.1 \pm 0.2 \times 10^{-21}$	158.76 ± 0.01	u
VCC 1869	$-6. \pm 7. \times 10^{-22}$	417.8	$2.3 \pm 0.8 \times 10^{-21}$	157.81 ± 0.03	u
VCC 1972	$2.04 \pm 0.01 \times 10^{-19}$	1083.4	$1.83 \pm 0.02 \times 10^{-19}$	158.585 ± 0.002	
		647.9	$1.1 \pm 0.2 \times 10^{-20}$	157.86 ± 0.02	g
VCC 1987	$3.03 \pm 0.02 \times 10^{-19}$	1135.8	$3.07 \pm 0.03 \times 10^{-19}$	158.371 ± 0.002	
VCC 2070	$3.4 \pm 0.1 \times 10^{-20}$	1120.8	$1.2 \pm 0.2 \times 10^{-20}$	158.24 ± 0.03	
VBACK01	$1.98 \pm 0.09 \times 10^{-20}$	244.6	$1.5 \pm 1.2 \times 10^{-21}$	157.5	u
VBACK03	$-4.2 \pm 0.8 \times 10^{-21}$	1014.2	$2.7 \pm 1.9 \times 10^{-21}$	157.6 ± 0.1	u
VBACK04	$2.19 \pm 0.08 \times 10^{-20}$	433.8	$2.5 \pm 1.3 \times 10^{-21}$	158.05 ± 0.04	
VBACK12_1	$-1.96 \pm 0.07 \times 10^{-20}$	843.7	$2.9 \pm 1.5 \times 10^{-21}$	157.92 ± 0.07	u
VBACK12_2	$6.4 \pm 0.5 \times 10^{-21}$	467.7	$1.2 \pm 0.5 \times 10^{-21}$	156.99 ± 0.03	u
VBACK13	$-8.8 \pm 1.1 \times 10^{-21}$	898.0	$3 \pm 3 \times 10^{-21}$	157.8 ± 0.1	u

Notes:
u upper limit based on strongest feature in spectrum.
g galactic [C II] emission.
2 Two measurements were made of this object. This second observation was a mispointed background observation.